Biochemical and Biophysical Research Communications 425 (2012) 25–32

Contents lists available at SciVerse ScienceDirect

Biochemical and Biophysical Research Communications

journal homepage: www.elsevier.com/locate/ybbrc

Cloning and characterization of the human *SH3BP2* promoter

Chun Fan [a,*], Robert J. Gaivin [a], Thomas A. Marth [a], Belinda Willard [b], Michael A. Levine [c], Steven A. Lietman [a,d,*]

[a] Department of Biomedical Engineering, The Cleveland Clinic, Cleveland, OH, USA
[b] Proteomics Laboratory, The Cleveland Clinic, Cleveland, OH, USA
[c] Division of Endocrinology, The Children's Hospital of Philadelphia and University of Pennsylvania School of Medicine, Philadelphia, PA, USA
[d] Department of Orthopaedic Surgery, The Cleveland Clinic, Cleveland, OH, USA

ARTICLE INFO

Article history:
Received 17 June 2012
Available online 17 July 2012

Keywords:
SH3BP2
Promoter
PARP1
Regulation

ABSTRACT

SH3BP2 activating mutations lead to an unique clinical condition in which patients develop symmetrical bone resorptive lesions of the jaw, a condition termed cherubism. Due to this specific temporal sequence and location of bone resorption, we investigated the transcriptional regulation of SH3BP2 expression. Analyses of 5′- and 3′-serial promoter deletions defined the core promoter/regulatory elements, including two repressor sites (from −1,200 to −1,000 and from +86 to +115, respectively) and two activator sites (a PARP1 binding site from −44 to −21 and a second activator site from +57 to +86). We identified that PARP1 binds to DNA from −44 to −21 by Streptavidin–biotin purification and confirmed this binding by electrophoretic mobility shift assay (EMSA). Mutagenesis of the PARP1 binding site on the *SH3BP2* promoter showed that this binding site is essential for SH3BP2 expression. EMSA and chromatin immunoprecipitation (ChIP) assays confirmed that PARP1 was able to bind to the *SH3BP2* promoter *in vitro* and *in vivo*. Indeed, knockout of *Parp1* in mice BMMs reduced expression of SH3BP2. These results demonstrate that PARP1 regulates expression of SH3BP2.

Published by Elsevier Inc.

1. Introduction

SH3BP2 activating mutations lead to an unique clinical condition in which patients develop symmetrical bone resorptive lesions of the jaw, a condition termed cherubism [1,2]. Experimental evidence has shown that these *SH3BP2* mutations lead to increased NFAT and TRAP activation with consequent increased osteoclastogenesis [2–5]. In addition, *SH3BP2* mutations present in cherubism have been shown to induce expression of other markers of osteoclastogenesis [6]. Preliminary evidence that these cherubism mutations are activating (rather than inactivating) derives from the fact that heterozygous deletion of the *SH3BP2* gene, in Wolf-Hirschhorn disease, does not lead to a bone resorptive phenotype [1–6]. Curiously, despite the mutations in *SH3BP2* being germline and widespread SH3BP2 expression, the bone lesions in cherubism are restricted to the jaw; and these lesions show a consistent temporal clinical pattern, with development at 3–5 years of age and quiescence or resolution after puberty.

Poly(ADP-ribose) polymerase (PARP) is a nuclear zinc finger DNA-binding protein that detects DNA strand breaks [7]. PARPs have been shown to be involved in DNA damage repair, cell death, transcription and chromatin modification/remodeling. Moreover PARPs have been implicated in a wide range of human diseases and are an important target for anti-cancer therapies. To date, 16 PARP isoforms have been identified including: PARP1, PARP2, PARP3, PARP4 (Vault-PARP), PARP5 (Tankyrase), PARP7 and PARP10; and each isoform has different functions [8–11]. PARP1, the best characterized member, works as a DNA damage nick-sensor protein that uses beta-NAD(+) to form polymers of ADP-ribose and has been implicated in DNA repair, chromatin modulation, insulation and enhancer-binding [8,12,13].

PARP enzymes play an important role in the pathogenesis of several diseases, such as, stroke, myocardial infarction, circulatory shock, diabetes, neurodegenerative disorders, including Parkinson's and Alzheimer diseases, allergy, colitis and other inflammatory disorders [8]. PARP5s (Tankyrase 1 and 2) have been shown to have a role in the pathogenesis of cherubism by binding to the wild-type SH3BP2 and thereby increasing SH3BP2 ubiquitination and subsequent degradation of the wild-type and by their relative inability to bind to the mutant form of SH3BP2 found in cherubism [9–11].

Increased knowledge about the control of SH3BP2 expression could not only lend insight into the pathophysiology of cherubism but also might provide a window into the molecular mechanisms involved in osteoclastogenesis and by inference osteoporosis in general.

* Corresponding authors. Address: Department of Biomedical Engineering, The Cleveland Clinic, 9500 Euclid Avenue, Cleveland, OH 44195, USA. Fax: +1 216 445 6255.
E-mail addresses: chunf@ccf.org (C. Fan), lietmas@ccf.org (S.A. Lietman).

0006-291X/$ - see front matter Published by Elsevier Inc.
http://dx.doi.org/10.1016/j.bbrc.2012.07.043

2. Methods

2.1. 5′-Rapid amplification cDNA ends (RACE)

Rapid amplification of cDNA ends (RACE) was performed with the 5′-Full RACE Kit (TaKaRa). Briefly, total RNA was purified from mononuclear cells from healthy donated human bone marrow cells after Ficoll gradient. First strand cDNA synthesis was performed using 5 μg of total RNA and 10 pmol of human *SH3BP2* gene specific primer 5′-CAAGGGCAGGTCTTTCTTTTCGTGGAA-3′ and subsequent circularization was by T4 ligase. Circular cDNAs were amplified by nested PCR with high fidelity Tag DNA polymerase (Roche). The nested PCR products were sub-cloned for DNA sequencing.

2.2. Generation of promoter constructs, transient transfection, and reporter gene assays

A 2.0 kb fragment containing the 5′-untranslated region of *SH3BP2* was generated from the bacterial artificial chromosome (clone RP11–808B21) by PCR and cloned into the pGL4.17 vectors (Promega, Madison, WI), and the generated plasmid was designated −2 kb *SH3BP2*p-LUC. Further deletions were created based on the −2 kb-*SH3BP2*p-LUC reporter gene using a PCR-based method. All constructs were verified by DNA sequencing.

RAW264.7 cells were transiently co-transfected using Nanojuice Transfection kit (Novagen, Madison, WI) with a luciferase reporter plasmid plus pRenilla-LUC plasmid to correct for variable transfection efficiency.

Bone marrow macrophages (BMMs) cells were obtained from *Parp1*-deficient 129/SvImJ mice (Jackson Laboratory). BM cells were flushed from the femurs and tibias of 8-week-old *Parp1* (-/-) mice or control mice 129/SvImJ (Jackson Laboratory), and resuspended in complete RPMI supplemented with 50 ng/ml recombinant M-CSF (R&D Systems). Nucleofections of BMMs were performed as described in the Mouse Macrophage Nucleofector kit (Amaxa Biosystems).

2.3. Emsa

EMSA was carried out as previously described [14–16]. Binding reactions were allowed to proceed at room temperature for 30 min in 10 mM HEPES, 100 ng poly(dIdC) (Sigma–Aldrich), with ^{32}P-labeled probes (IDT Technologies, Coralville, IA), and 1–5 μg RAW264.7 cell nuclear extract (NE). For the non-radioisotope EMSA, 0.5 pM of probe and 0.1–1 μl *in vitro* translated PARP1 protein were used in the binding reaction. Samples were analyzed by 5–10% native PAGE.

2.4. Streptavidin–biotin purification of the DNA binding protein from RAW264.7 cells

10 pM biotin-labeled double stranded GC-box III probe (Sigma–Aldrich) was incubated with 10 mg of RAW264.7 NE in EMSA binding buffer as above described. Protein bound to the GC-box III probe was pulled down using Streptavidin MagneSphere Paramagnetic Particles (Promega, Madison, WI), and after washing with binding buffer, 2 × SDS sample buffer was added and heated at 96 °C, DNA–protein complex was separated by SDS–PAGE and silver staining gel was used for mass spectrometry analysis.

2.5. Chromatin Immunoprecipitation

Chromatin immunoprecipitation (ChIP) assays were performed as described previously [14–16] according to manufacturer's instructions (Upstate, Lake Placid, NY) using 1–2 × 10^7 RAW264.7 cells. The amounts of target DNA bound to PARP1 was quantified using PCR. The ratio of a specific DNA fragment in each immunoprecipitation to the fragment in the DNA before immunoprecipitation (input DNA) was calculated from each Ct value.

2.6. Statistical analysis

We used Student's unpaired two-tailed *t*-test for all statistical analyses. Differences between groups were considered significant with a $p < 0.05$, and indicated with a single asterisk if $p < 0.05$ and double asterisks if $p < 0.01$.

3. Results

3.1. Identification of the human SH3BP2 gene transcription start sites

Identification and mapping of promoter regions are key aspects of gene regulatory studies and the precise localization of a gene promoter requires the determination of the transcription start site (TSS). We designate the position of the G residue as +1 throughout the text) (Fig. 1A). Further, analysis from Ace View databases indicated that exon 1B falls within the exons of a bone-expressed gene strongly predicted to translate 561 amino acids protein named SH3BP2.

We designed a reverse primer (R) based on a sequence in exon II (Fig. 1B). RT–PCR analysis of total RNA isolated from human bone marrow tissue with primer combinations F5/R and F6/R yielded amplicons, whereas other combinations did not produce any PCR product (Fig. 1C). These data suggest that the *SH3BP2* TSS is located in exon IB, not exon IA in human tissue. We carried out 5′-RACE analysis with total RNA isolated from human bone marrow donated from a healthy volunteer. The nested PCR yielded a single DNA fragment (Fig. 1D) that was cloned and sequenced. The TSS was identified by sequence analysis and mapped upstream of the *SH3BP2* coding region inside exon b1B.

3.2. Identification of a cis-acting DNA element from −108 to +86 that increases transcription of SH3BP2

After mapping of the TSS, a series of nine 5′-deletions were created for *SH3BP2* promoter analysis from the 2 kb *SH3BP2*p-LUC construct in the pGL4.17 promoter-less luciferase vector (Fig. 2A). The deletions were transiently transfected into RAW264.7 cells, and transcription activity was measured as a function of luciferase activity. RAW264.7 cells were used here as they are a preosteoclastic cell line. In addition experiments with the RAW264.7 cell line have accurately predicted the effect of SH3BP2 on bone marrow macrophages and the phenotype of knockin and knockout *Sh3bp2* mice [17–21]. Compared with the promoter-less reporter, the full-length −2,000 *SH3BP2*p-LUC reporter exhibited a 15-fold increase in luciferase activity (Fig. 2A).

Removal of sequences between −2,000 and −1,000 increased transcription of the *SH3BP2* promoter by 3.5-fold, suggesting the presence of a cis-acting repressor element in this region that represses expression of SH3BP2. Removal of the sequences from −1,000 to −200 did not change transcriptional activity, indicating that the basal element within the promoter/regulatory region of *SH3BP2* is in the −200 bp region.

To map the region responsible for the basal promoter activity, an additional three 3′-serial promoter truncations, were created and analyzed (Fig. 2B). Removal of the sequence between +86 to +115 increased transcription of the *SH3BP2* promoter 16-fold, suggesting the presence of a cis-acting repressor element in this region. Removal of the sequence between +57 to +86 reduced *SH3BP2* promoter activity 2.5-fold, indicating the presence of a weak activator in this region (Fig. 2B). These data suggest that the basal promoter of *SH3BP2* is located between −200 and +86

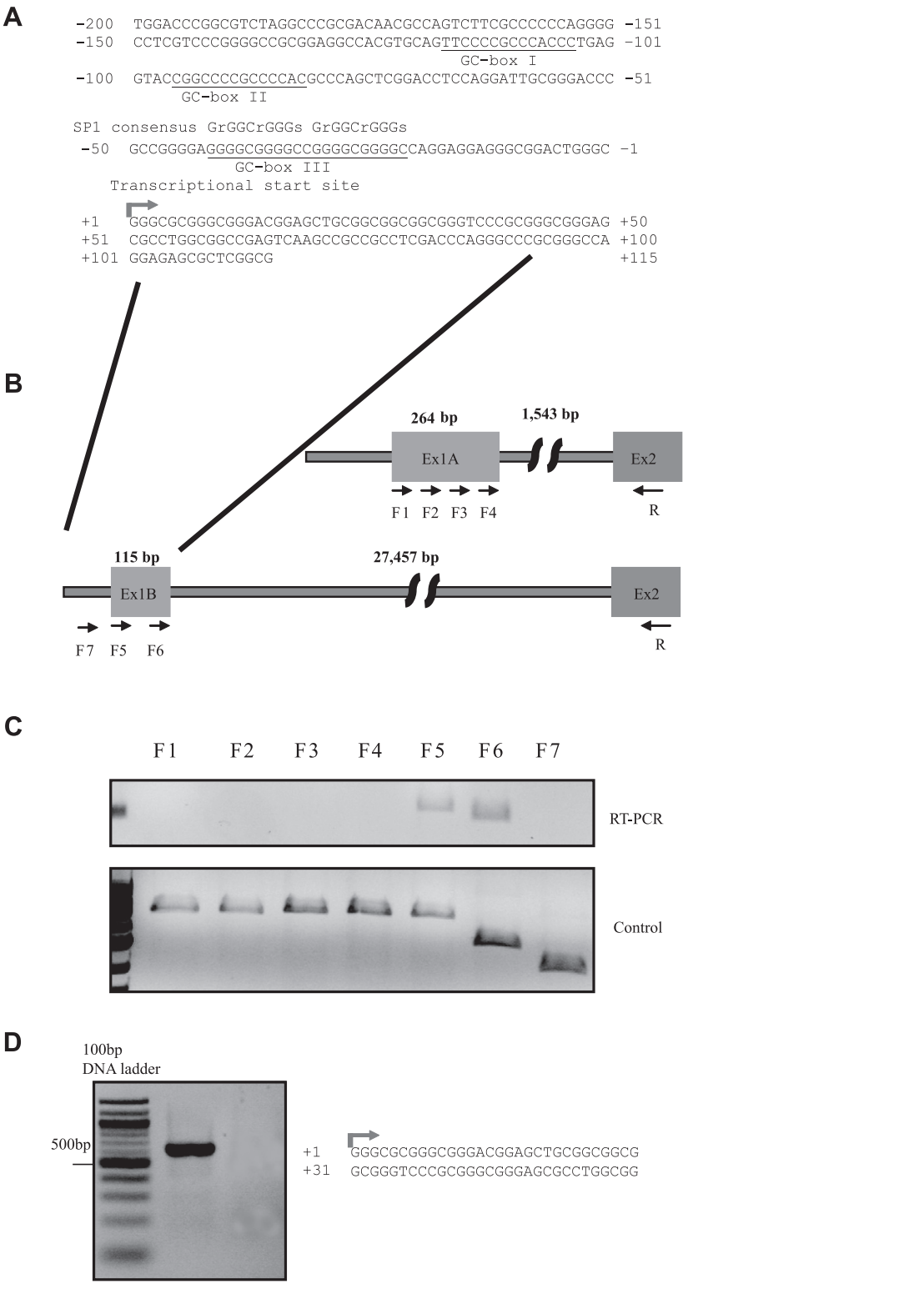

Fig. 1. Mapping of the transcription start site of the *SH3BP2* gene. (A) The nucleotide sequence of the human *SH3BP2* promoter/regulatory region is shown. (B) Representation of the two longer transcript transcription start sites of the *SH3BP2* gene. (C) Identification of the putative TSS of *SH3BP2* by RT–PCR analysis. The *top panel* shows results from RT–PCR, and the *bottom panel* shows positive control PCR primers (regular PCR with genomic DNA). (D) 5′-RACE followed by nested PCR product from circularized cDNA (left). A water control with no DNA served as a negative control (right).

from the transcription start site, which was consistent with our earlier results. Deletion of the region from −68 to −21, greatly reduced *SH3BP2* promoter activity compared to baseline (Fig. 2C), suggesting a strong activator in this region. Taken together this suggested that the core promoter of *SH3BP2* is located in the region from −68 to +86, encompassing the two activators (Figs. 2B and C).

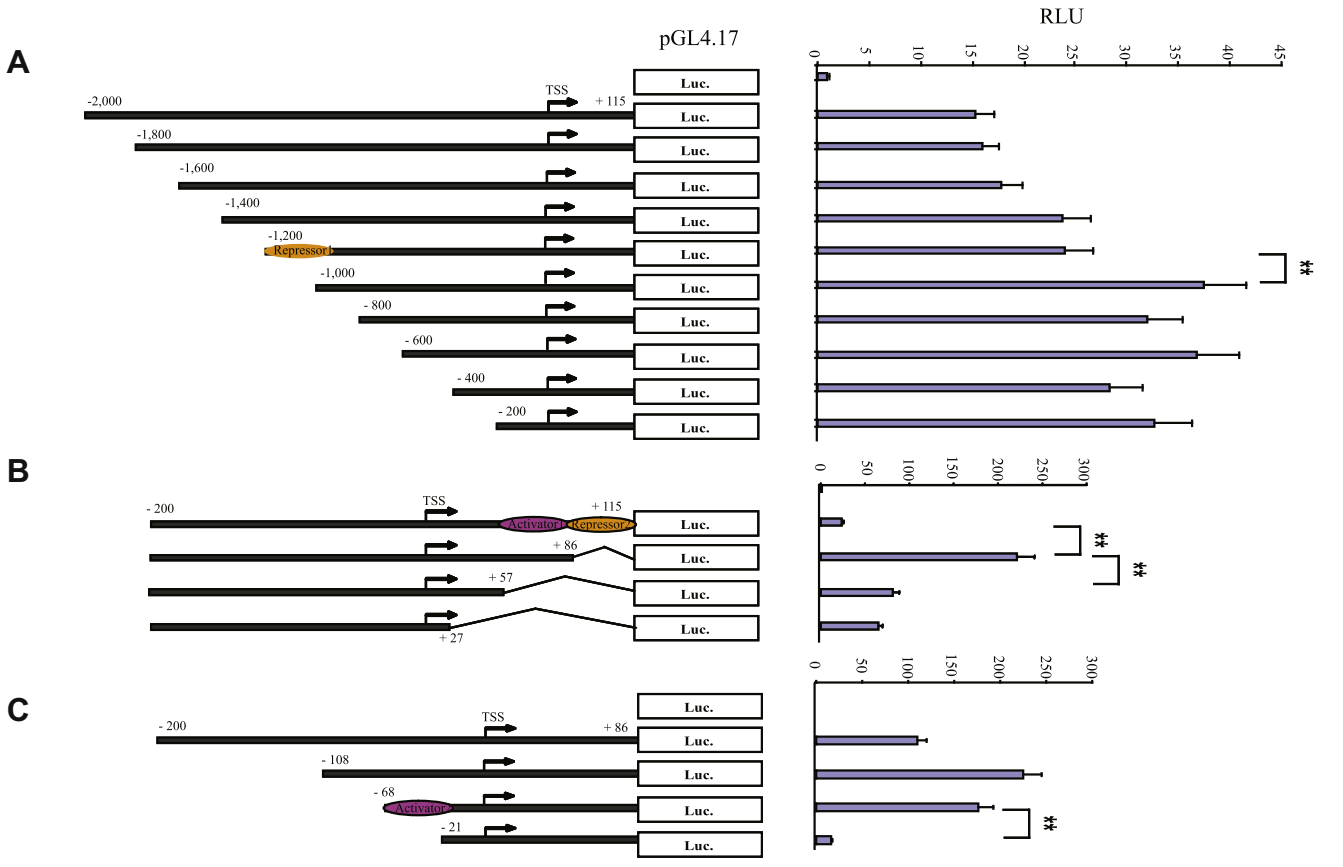

Fig. 2. Deletion analysis of the human *SH3BP2* promoter and fine mapping of the *SH3BP2* transcription factor binding site. (A) Schematic representation of the *SH3BP2* promoter luciferase reporter. (B) Serial 3′-deletion was generated based on −2,000 bp to +115 bp-*SH3BP2*p-LUC. The locations of activator or repressor sites (olive-shaped) are indicated. (C) Further 5′-deletions were created based on −200 bp to +86 bp-*SH3BP2*p-LUC. The relative luciferase activity of each deletion mutant in RAW264.7 cells is shown on the right. Data shown represent three independent experiments. (D) Probes used for EMSA and mutagenesis are shown. (E) DNA–protein complexes from incubation of oligonucleotides with RAW264.7 lysates were detected with the EMSA probe, particularly in the GC-box II and III regions. (F) The functional identification of binding proteins to the *SH3BP2* promoter region is shown. The relative luciferase activity of each mutant in RAW264.7 cells is shown on the right. Data represent three independent experiments. GC-II: GC-box II site; GC-III: GC-box III site.

3.3. Identification of a functional binding site in the promoter/regulatory region of SH3BP2

As Fig. 1A shows, in human *SH3BP2* there are three GC-boxes in the promoter/regulatory region. To verify whether these three areas were capable of protein binding, an EMSA was performed using double-stranded oligonucleotides from the GC-box I, II, and III regions (Fig. 2D) and RAW264.7 cell nuclear extract (NE). Incubation of NE from RAW264.7 cells with ^{32}P-labeled probes resulted in the formation of DNA–protein complexes with the GC-box II and III oligonucleotides, and the most protein binding was to the GC-box III oligonucleotide (Fig. 2E).

3.4. GC-box III site is essential for expression of SH3BP2

To explore the GC-box III binding site's functional significance, a mutant of this site was found to reduce SH3BP2 expression to nearly basal levels, however mutation of the GC-box II site did not change SH3BP2 expression (Fig. 2F). Mutation of both sites abolished transcription activity of the *SH3BP2* promoter to nearly basal levels. These data suggest that the GC-box III region, not GC-box II, is essential for expression of SH3BP2.

3.5. PARP1 interacts directly with the SH3BP2 promoter in RAW264.7 cells

EMSAs were performed using a double-stranded oligonucleotide encompassing the region from −44 to −21 (Fig. 2D) with RAW264.7 cell NE. Incubation of RAW264.7 cell NE with the ^{32}P-labeled GC-box III probe resulted in the formation of a DNA–protein complex (Fig. 3A) similar to EMSA1 (Fig. 2E). The DNA–protein interaction appeared to be specific because it was eliminated by the addition of 100-fold excess unlabeled GC-box III probe but was not affected by the addition of 100-fold excess mutant oligonucleotide. The specific DNA–protein complex was not shifted in EMSA3 by using NE preincubated with an anti-SP1 antibody, or negative control IgG (Fig. 3B). These data suggest that, although the GC-box III site is a putative SP1 consensus binding site [22], SP1 is not binding here.

We therefore used a proteomics approach to identify candidate proteins as PARP1 (Fig. 3D). *In vitro* translated PARP1 protein (Fig. 3E) also bound to sense and double stranded GC-box III (Fig. 3F). Quantification assay showed that PARP1 bound to DNA in a dose dependent manner (Fig. 3G). Supershift EMSA (Fig. 3H) confirmed that the GC-box III binding protein was PARP1 in RAW264.7 cells.

3.6. PARP1 transactivates the SH3BP2 promoter

Transfection of the PARP1 expression construct into RAW264.7 cells resulted in markedly increased activation of the *SH3BP2* promoter compared with the empty expression vector (Fig. 3I). GC-box III mutant had dramatically reduced transcription activity, PARP1 inhibitor 3-AB also reduced PARP1-dependent transcriptional activity of the *SH3BP2* promoter. These results indicate that transactivation of the *SH3BP2* promoter requires the presence of the DNA binding site for PARP1.

To verify that native PARP1 protein bound to the *SH3BP2* promoter *in vivo*, a conventional ChIP assay was performed using a specific monoclonal PARP1 antibody and specific primers for the *SH3BP2* promoter. Using RAW264.7 cell extracts transiently transfected with a PARP1 plasmid, PARP1 specifically bound to the *SH3BP2* promoter (Fig. 3J). Taken together, these data confirm that PARP1 can interact with a cis-DNA element in the *SH3BP2* promoter/regulatory region.

3.7. Parp1 (-/-) in mice reduced SH3BP2 core promoter activity and SH3BP2 protein synthesis

To elucidate the role of PARP1 in the regulation of the *SH3BP2* gene *in vivo*, we analyzed core *SH3BP2* promoter activity and SH3BP2 protein expression in *Parp1* (-/-) mice BMMs. Transfection experiments were performed using the core −108/+86-*SH3BP2*p-LUC construct or an empty expression vector as control. Transfection of the core −108/+86-*SH3BP2*p-LUC construct demonstrated markedly increased luciferase activity compared with the empty expression vector in wild type mice BMMs. In contrast, no luciferase activity was detected with the pGL4.17 (promoterless) luciferase vector and the core −108/+86-*SH3BP2*p-LUC construct dramatically reduced transcription activity in *Parp1* (-/-) mice BMMs by 81.3% compare to wild type BMMs (Fig. 4A). Immunoblot analysis revealed (Fig. 4B) that the expression level of SH3BP2 was decreased in *Parp1* (-/-) BMMs by 79.6% compare to wild type BMMs (Fig. 4C). Taken together, these data confirm that PARP1 can interact with a cis-DNA element in the *SH3BP2* promoter/regulatory region and regulates the expression of *SH3BP2 in vivo*.

4. Discussion

SH3BP2 plays a role in osteoclastogenesis and *SH3BP2* mutations are associated with bone resorptive tumors with a specific temporal onset and location in the jaw in patients with cherubism [1,23–25]. In addition in a mouse knock-in model, with a mutation found in cherubism, there are bone resorptive tumors in many skeletal locations [26]. We therefore characterized the *SH3BP2* promoter/regulatory region to gain insight into the regulation of *SH3BP2* expression. The *SH3BP2* promoter has several interesting features: first, it lacks a TATA box and has 3 transcript variants. Thus, the *SH3BP2* promoter joins a growing list of osteoclastogenesis genes that use a TATA-less promoter and possess multiple, closely spaced transcription initiation sites [27,28]. Second, the sequences flanking the TSS (transcription start site) and translation start site of the *SH3BP2* gene are C/G-rich (81%) and contain more than 42 *CpG* islands which are targets for gene regulation by DNA methylation [29,30]. Methylation may be one mechanism by which the expression of the *SH3BP2* gene is regulated at the pre-transcription level. Third, the *SH3BP2* gene uses a functionally analogous initiator element (first described for the terminal deoxytransferase gene promoter to direct transcription initiation) [31].

The region 200 bp upstream of the TSS has three GC-box canonical SP1 consensus sites GrGGCrGGGs (r = A or G; s = C or G), and the third region (GC-box III, the −44 bp to −21 bp PARP1 binding site) consists of the SP1 variant: GGGGCGGGGC [22]. Interestingly, this variant sequence apparently bound PARP1 but not SP1, as demonstrated by the supershift assay with SP1 (Fig. 3B) and PARP1 antibodies (Fig. 3H). PARP1 also bound to sense or double stranded DNA from the GC box III region and not the antisense DNA from this region indicating orientation specific binding and that PARP1 does not bind nonspecifically to DNA break points (Fig. 3D). *In vitro* translated PARP1 protein bound to the GC box III DNA (Fig. 3F) in a similar manner to that of PARP1 in RAW264.7 NE. These data strongly demonstrate that PARP1 binding to the GC-rich box III region is direct and with orientation specificity.

Point mutations in the coding region of *SH3BP2* are associated with cherubism [1,24]. Now that we have characterized the promoter/regulatory region of *SH3BP2*, future studies are needed to test whether there is an association between polymorphisms, mutations or methylation changes in the *SH3BP2* promoter and cherubism. Such promoter changes, could explain the presence of cherubism in patients without mutations in the *SH3BP2* coding re-

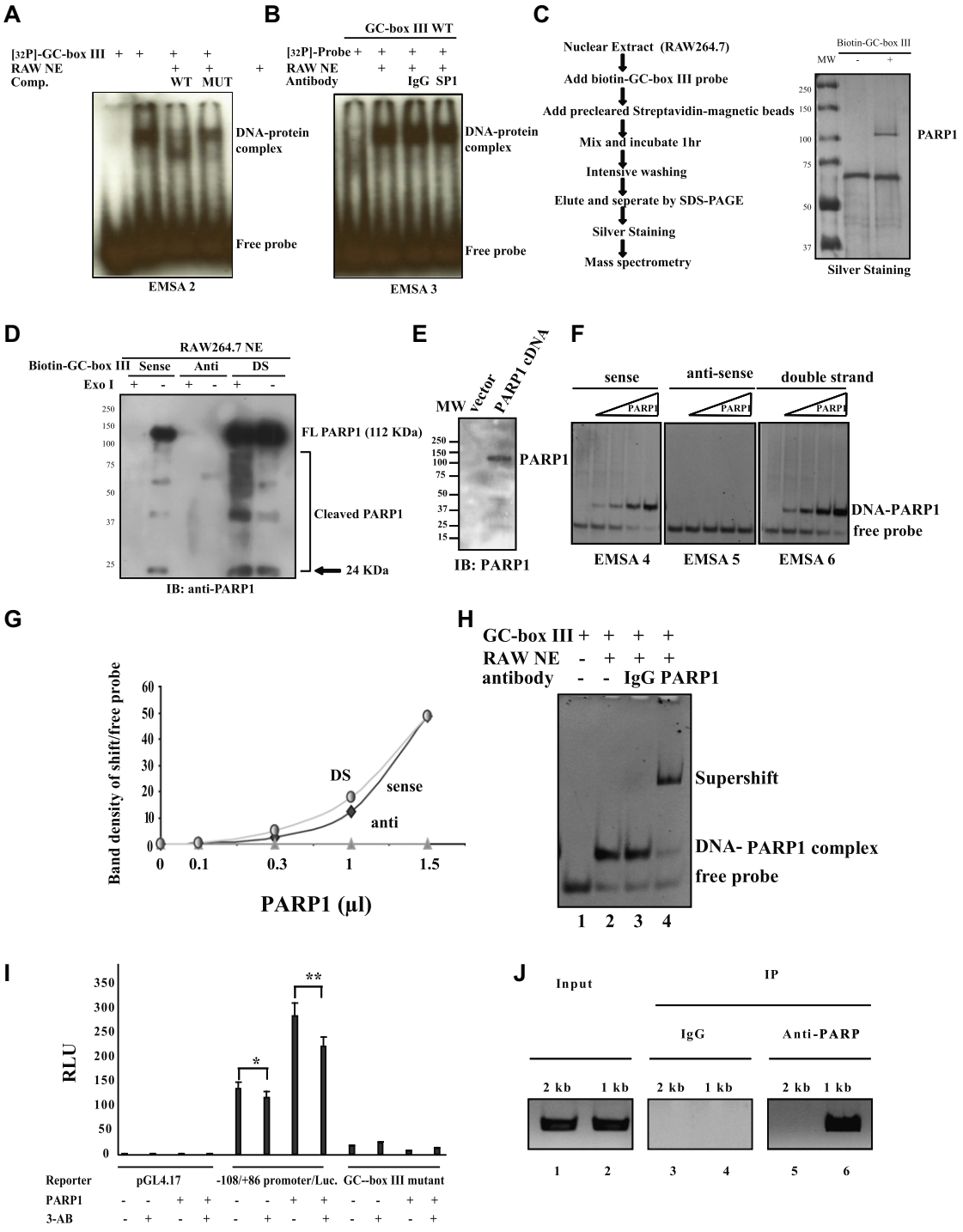

Fig. 3. The PARP1 binds to the *SH3BP2* core promoter and PARP1 is required for maximal *SH3BP2* promoter activity. (A) EMSA data is shown, with ^{32}P-labeled GC-box III probe incubated with (lanes 2–4) or without (lane 1) nuclear extract from RAW264.7 cells. In lanes 3 and 4, there was preincubation of a 100× excess of cold competitor WT or mutant GC-box III probe, respectively. (B) Supershift EMSA is shown with (lanes 2–4) or without (lane 1) nuclear extract from RAW264.7 lysates. (C) Streptavidin–biotin purification of the PARP1 protein from RAW264.7 cells after binding to the *SH3BP2* promoter *in vivo* is shown. (D) Confirmation of PARP1 as a DNA binding protein is demonstrated by immunoblot. Single stranded sense or antisense, or double stranded GC-box III probes with (lane 1, 3, 5) or without (lane 2, 4, 6) Exo I (hydrolysis of single stranded DNA) were used for this experiment. FL indicates full length. (E) Immunoblotting of *in vitro* translated human PARP1 protein is shown. (F) EMSA assay of unlabeled GC-box III probe binding to full length PARP1 protein. Sense (EMSA4) and double stranded (EMSA6) probes bound PARP1 in a dose-dependent manner, while anti-sense (EMSA5) probe binding is not detected in these experiments. (G) Quantification of PARP1 binding is shown based on three independent experiments ($n = 3$). DNA was stained with ethidium bromide and the ratio of band densities of shift/free probe were plotted. DS, double stranded probe. (H) Supershift EMSA is shown with (lanes 2–4) or without (lane 1) RAW264.7 nuclear extract (RAW NE). (I) Overexpression of PARP1 increased expression of SH3BP2 and PARP1 inhibitor 3-AB inhibited the transcriptional activation of the *SH3BP2* promoter. Transcriptional activity for wild-type and GC-box III mutant −108/+86-*SH3BP2*p-LUC reporter genes (left panel) are shown. RAW264.7 cells with or without RANKL treatment were co-transfected with a reporter gene and pcDNA3.1-PARP1 mammalian expression plasmid. (J) ChIP analysis detected binding of the PARP1 protein to the 2 kb *SH3BP2* promoter *in vivo* in RAW264.7 cells. Primers amplifying the *SH3BP2* promoter were used for the PCR analysis. For the 1 kb analysis, ChIP with PCR primers covering the *SH3BP2* promoter fragment (with the PARP1 binding site located within the 1 kb region upstream from the transcription start site) were used; and for the 2 kb analysis, ChIPs with PCR primers covering other *SH3BP2* promoter fragments without the PARP1 binding site were used.

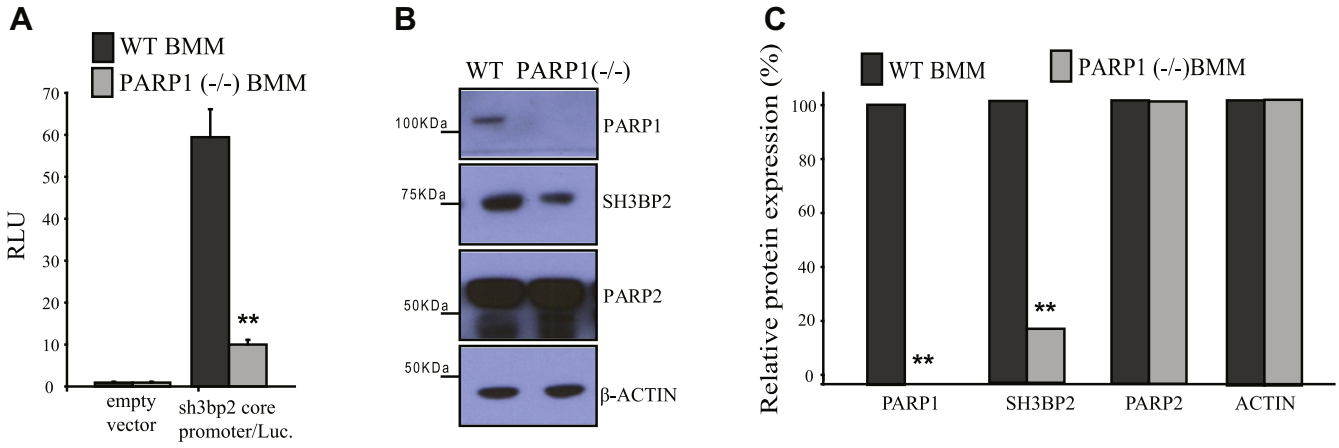

Fig. 4. Knockout of PARP1 reduced the activity of core *SH3BP2* promoter and SH3BP2 protein synthesis *in vivo*. (A) Luciferase reporter assay. BMMs were electroporated with the core *SH3BP2* promoter/Luc. reporter or empty vector pGL4.17. Data shown represent two independent experiments with the luciferase activity in triplicate. (B) Immunoblot demonstrates the expression levels of PARP1, SH3BP2, PARP2 and β-ACTIN in WT and *Parp1* (-/-) BMMs. (C) Quantification was based on two independent experiments ($n = 2$). Immunoblot analysis shows that *Parp1* (-/-) reduced expression of SH3BP2. β-ACTIN or PARP2 served as a loading control.

gion and or the large differences in phenotype in brothers with the same mutation (personal communication Sven Kreiborg) [24].

In conclusion, the present study is the first to define the TSS and map the regulatory motifs within the *SH3BP2* promoter/regulatory region. Moreover we define the molecular mechanism for the transcriptional regulation of the expression of the *SH3BP2* gene. Specifically, we have identified PARP1 as a key regulator of the *SH3BP2* gene.

Acknowledgments

This work was supported by in part by US Public Health Service Research Grants K08-AR47661 (SAL), R01-DE018237 (SAL) and R01DE018237-02S1 (SAL, TM). Dr. Lietman is the recipient of by a Career Development Award from the Orthopaedic Research and Education Foundation.

References

[1] Y. Ueki, V. Tiziani, C. Santanna, N. Fukai, C. Maulik, J. Garfinkle, C. Ninomiya, C. Amaral, H. Peters, M. Habal, L. Rhee-Morris, J.B. Doss, S. Kreiberg, B.R. Olsen, E. Reichenberger, Mutations in the gene encoding c-Abl-binding protein SH3BP2 cause cherubism, Nat. Genet. 28 (2001) 125–126.
[2] A.D. Bergemann, F. Cole, K. Hirschhorn, The etiology of Wolf-Hirschhorn syndrome, Trends Genet. 21 (2005) 188–195.
[3] A. Battaglia, J.C. Carey, Health supervision and anticipatory guidance of individuals with Wolf-Hirschhorn syndrome, Am. J. Med. Genet. 89 (1999) 111–115.
[4] A. Battaglia, J.C. Carey, P. Cederholm, D.H. Viskochil, A.R. Brothman, C. Galasso, Natural history of Wolf-Hirschhorn syndrome: experience with 15 cases, Pediatrics 103 (1999) 830–836.
[5] W. Sepulveda, Prenatal 3-dimensional sonographic depiction of the Wolf-Hirschhorn phenotype - the « greek warrior helmet » and « tulip » signs, J. Ultrasound Med. 26 (2007) 407–410.
[6] M.M. Carrasquillo, A.S. McCallion, E.G. Puffenberger, C.S. Kashuk, N. Nouri, A. Chakravarti, Genome-wide association study and mouse model identify interaction between RET and EDNRB pathways in hirschsprung disease, Nat. Genet. 32 (2002) 237–244.
[7] C. Trucco, F.J. Oliver, G. de Murcia, J. Menissier-de Murcia, DNA repair defect in poly(ADP-ribose) polymerase-deficient cell lines, Nucleic Acids Res. 26 (1998) 2644–2649.
[8] C.A. de la Lastra, I. Villegas, S. Sanchez-Fidalgo, Poly(ADP-ribose) polymerase inhibitors: new pharmacological functions and potential clinical implications, Curr. Pharm. Des. 13 (2007) 933–962.
[9] A.D. Berendsen, Tankyrase loses its grip on SH3BP2 in cherubism, Cell 147 (2011) 1222–1223.
[10] N. Levaot, Loss of tankyrase-mediated destruction of 3BP2 is the underlying pathogenic mechanism of cherubism, Cell 147 (2011) 1324–1339.
[11] D.V. Novack, Jawing about TNF: new hope for cherubism, Cell 128 (2007) 15–17.
[12] W.L. Kraus, Transcriptional control by PARP-1: chromatin modulation, enhancer-binding, coregulation, and insulation, Curr. Opin. Cell Biol. 20 (2008) 294–302.
[13] J. Yelamos, J. Farres, L. Llacuna, C. Ampurdanes, J. Martin-Caballero, PARP-1 and PARP-2: new players in tumour development, Am. J. Cancer Res. 1 (2011) 328–346.
[14] C. Fan, P. Ouyang, A.A. Timur, P. He, S.A. You, Y. Hu, T. Ke, D.J. Driscoll, Q.Y. Chen, Q.K. Wang, Novel roles of GATA1 in regulation of angiogenic factor AGGF1 and endothelial cell function, J. Biol. Chem. 284 (2009) 23331–23343.
[15] C. Fan, Q.Y. Chen, Q.K. Wang, Functional role of transcriptional factor TBX5 in pre-mRNA splicing and holt-oram syndrome via association with SC35, J. Biol. Chem. 284 (2009) 25653–25663.
[16] C. Fan, M.G. Liu, Q. Wang, Functional analysis of TBX5 missense mutations associated with holt-oram syndrome, J. Biol. Chem. 278 (2003) 8780–8785.
[17] S.A. Lietman, L.H. Yin, M.A. Levine, SH3BP2 is an activator of NFAT activity and osteoclastogenesis, Biochem. Biophys. Res. Commun. 371 (2008) 644–648.
[18] Y. Ueki, C.Y. Lin, M. Senoo, T. Ebihara, N. Agata, M. Onji, Y. Saheki, T. Kawai, P.M. Mukherjee, E. Reichenberger, B.R. Olsen, Increased myeloid cell responses to M-CSF and RANKL cause bone loss and inflammation in SH3BP2 « cherubism » mice, Cell 128 (2007) 71–83.
[19] S.A. Lietman, L.H. Yin, M.A. Levine, SH3BP2 mutations potentiate osteoclastogenesis via PLC gamma, J. Orthop. Res. 28 (2010) 1425–1430.
[20] N. Levaot, P.D. Simoncic, I.D. Dimitriou, A. Scotter, R.J. La, A.H. Ng, T.L. Willett, C.J. Wang, S. Janmohamed, M. Grynpas, E. Reichenberger, R. Rottapel, 3BP2-deficient mice are osteoporotic with impaired osteoblast and osteoclast functions, J. Clin. Invest. 121 (2011) 3244–3257.
[21] T. Kawamoto, C. Fan, R.J. Gaivin, M.A. Levine, S.A. Lietman, Decreased SH3BP2 inhibits osteoclast differentiation and function, J. Orthop. Res. 29 (2011) 1521–1527.
[22] M. Mucha, L. Ooi, J.E. Linley, P. Mordaka, C. Dalle, B. Robertson, N. Gamper, I.C. Wood, Transcriptional control of KCNQ channel genes and the regulation of neuronal excitability, J. Neurosci. 30 (2010) 13235–13245.
[23] A. GuezGuez, V. Prod'homme, X. Mouska, A. Baudot, C. Blin-Wakkach, R. Rottapel, M. Deckert, 3BP2 adapter protein is required for receptor activator of NF kappa B ligand (RANKL)-induced osteoclast differentiation of RAW264.7 cells, J. Biol. Chem. 285 (2010) 20952–20963.
[24] S.A. Lietman, N. Kalinchinko, X. Deng, R. Kohanski, M.A. Levine, Identification of a novel mutation of SH3BP2 in cherubism and demonstration that SH3BP2 mutations lead to increased NFAT activation, Hum. Mutat. 27 (2006) 717–718.
[25] A.O. Aliprantis, Y. Ueki, R. Sulyanto, A. Park, K.S. Sigrist, S.M. Sharma, M.C. Ostrowski, B.R. Olsen, L.H. Glimcher, NFATc1 in mice represses osteoprotegerin during osteoclastogenesis and dissociates systemic osteopenia from inflammation in cherubism, J. Clin. Invest. 118 (2008) 3775–3789.
[26] P. Mukherjee, T. Jafarov, Y. Ueki, A.L. Boskey, B.R. Olsen, E.J. Reichenberger, Characterization of Sh3bp2 knock-in mice - a model for cherubism, J. Bone Miner. Res. 21 (2006) S80.
[27] S.T. Smale, Transcription initiation from TATA-less promoters within eukaryotic protein-coding genes, Biochim. Biophys. Acta, Gene Struct. Expression 1351 (1997) 73–88.
[28] B.M. Badran, K. Kunstman, J. Stanton, M. Moschitta, A. Zerghe, H. Akl, A. Burny, S.M. Wolinsky, K.E. Willard-Gallo, Transcriptional regulation of the human CD3 gamma gene: the TATA-less CD3 gamma promoter functions via an initiator and contiguous Sp-binding elements, J. Immunol. 174 (2005) 6238–6249.

[29] A.P. Feinberg, B. Vogelstein, Hypomethylation of ras oncogenes in primary human cancers, Biochem. Biophys. Res. Commun. 111 (1983) 47–54.
[30] A.P. Feinberg, B. Vogelstein, Hypomethylation distinguishes genes of some human cancers from their normal counterparts, Nature 301 (1983) 89–92.
[31] A. Barski, S. Cuddapah, K.R. Cui, T.Y. Roh, D.E. Schones, Z.B. Wang, G. Wei, I. Chepelev, K.J. Zhao, High-resolution profiling of histone methylations in the human genome, Cell 129 (2007) 823–837.